POLITECNICO
MILANO 1863

SCUOLA DI INGEGNERIA INDUSTRIALE
E DELL'INFORMAZIONE

Executive Summary of the Thesis

Study of Surface Electrocatalytic Processes by Ultrafast X-ray Diffraction

Laurea Magistrale in Physics Engineering - Ingegneria Fisica

Author: Meryem Ennaji

Advisor: Prof. Marco Moretti

Co-advisor: Dr. Jakub Drnec

Academic year: 2022-2023

1. Introduction

The energy transition stands as a major challenge in today's society. To mitigate global climate change, it is imperative to significantly reduce greenhouse gas emissions, which entails a gradual and continuous shift in global energy consumption from fossil-based sources to a zero-carbon system. In the field of sustainable energy technology today, nanostructured materials are pivotal in facilitating electrochemical reactions, with particular emphasis placed on Platinum nanoparticles (Pt NP). Platinum, in fact, assumes a critical role in electrochemistry as it stands as the most active element for numerous essential electrocatalytic reactions. Furthermore, in the context of electrochemical energy conversion and storage, such as in polymer electrolyte membrane fuel cells (PEMFCs), nanostructured materials such as platinum nanoparticles (Pt NPs) serve as catalysts in both the anode and cathode, enhancing those electrochemical reactions involved in generating electricity from hydrogen and oxygen in PEMFCs. In the case of heterogeneous catalysis, where the reactions occur onto the catalyst surface, the most promising approach in material design follows the Sabatier principle: the ability of the surface to bind adsorbates and the strength of the bonds define the reaction thermodynamics and kinetics [2]. In this respect, the present project has the objective of studying the kinetics of fast fundamental processes initial stage of metal electrooxidation taking place at the surface of nanostructured electrocatalyst electrodes. We will take advantage of the high brilliance 4th generation synchrotron source at ESRF for the fundamental understanding of the materials behavior under electrochemical conditions. We will focus mainly on: electric double layer restructuring and adsorption/desorption of small molecules.

1.1. Electric Double-Layer

The electric double layer (EDL) is is one of the focal point of electrochemistry, it is the most important region for electrochemical and heterogeneous catalysis. The first EDL model was proposed by Helmholtz in 1853. It is a very simple model but still relevant to describe charge separation and predicts the capacitance of EDL in a proper way. An electrode in contact with an electrolyte shows a gradient in the electrochemical potential at the interface between the two. An electron experiencing this gradient will be involved in charge transfer. Closest to the solid

electrode, a layer of ions forms that is strongly attracted to the electrode's surface due to the electrical potential, this region is named inner Helmholtz plane. Beyond the Helmholtz layer, there is a region where ions are distributed more loosely and not strongly bound to the electrode, this region is named outer Helmholtz plane. The separation between the two parallel planes is given by the counter-ion radius, yielding a capacitance that is larger than the typical value of a dielectric capacitor by many orders of magnitude. This is the reason why EDL capacitors hold great promise for the next generation of electrical energy storage.

1.2. Metal Oxidation and Oxide Film Formation

The oxidation of the Pt surface directly impacts the separate processes of Pt dissolution and oxygen reduction, lowering the longevity and efficiency of the Pt catalysts. When a metal is used at the electrode in an electrochemical cell and exposed to an electrolyte, oxidation reactions take place:

$$M \rightarrow M^z + ze^- \tag{1}$$

where M identifies the metal, z the metal's oxidation state and ze^- represents z moles of electrons. The products of this reaction is given by metal cations and electrons. By coupling this reaction with hydrolysis of the cations leads to the formation of a poorly adherent oxide film:

$$M^z + zH_20 \rightarrow MO_z^{2-} + 2H_2 \tag{2}$$

Dissolution refers to the process of metal atoms or ions leaving the metal surface and entering the surrounding electrolyte. This extraction process is a crucial step in the corrosion process. The dissolved metal cations then react with oxygen, water, or other chemical species in the environment, leading to the formation of metal oxide compounds on the metal surface. Moreover, when a mono layer of OH or O is formed on the metal surface in the form of a 2-dimensional array, field-dependent interchange between metal atoms in the surface and OH or 0 species in the ad-layer contribute to continuing oxidation and growth of the film. It is the so called place exchange phenomenon, a metal surface atom exchanges with an oxygen species [3].

2. Material and Methods

2.1. Polymer electrolyte membrane fuel cell

PEMFC is an electrochemical device that converts the chemical energy of hydrogen and oxygen directly into electrical energy. The core component of this fuel cell is a solid polymer electrolyte membrane. This membrane allows protons (hydrogen ions) to be transmitted from one face to the other while blocking electrons. There are two main electrochemical reactions that occur in this fuel cell. Once hydrogen (H_2) is supplied at the anode there's an oxidation process in which hydrogen molecules are split into protons (H^+) and electrons (e^-), the equation(3) represent the hydrogen oxidation reaction (HOR). The electrons are conducted through an external circuit generating electrical current and powering any connected devices or systems. The protons, as we already said, migrate to the cathode side passing through the membrane.
At the cathode side the reduction reaction takes place, the equation (4) is the oxygen reduction reaction (ORR). Indeed, air is supplied at the cathode side of the fuel cell, from air we get oxygen gas (O_2). Then, by combining oxygen molecules, protons, and electrons we produce water (H_2O), that with heat constitute the byproduct of the overall reaction.

$$Anode : H_2 \rightarrow 2H^+ + 2e^-, \tag{3}$$

$$Cathode : \frac{1}{2}O_2 + 2H^+ + 2e^- \rightarrow H_2O, \tag{4}$$

$$Overall : H_2 + \frac{1}{2}O_2 \rightarrow H_2O \tag{5}$$

2.2. Design of the Membrane Electrode Assembly

The central element within a fuel cell is known as the Membrane Electrode Assembly (MEA), comprising multiple layers of materials functioning collaboratively to enable electrochemical reactions.We can see the schematic structure of the MEA in Fig. 1. The heart of the MEA is the PEM, made of Nafion 112, it is a thin, 125 μm, and solide electrolyte that allows the passage of protons while blocking the flow of electrons. For this study the MEA was prepared by cutting CCM, catalyst coated membrane, into $25mm^2$ piece and laminating it into a larger Mylar frame. On one side of the CCM

there is the anode catalyst layer and on the other side there's the cathode catalyst layer, those two are both consisting of platinum nanoparticles supported on carbon. Indeed, the anode is carbon-supported Pt with 0.079 mgPt/cm2 loading, the cathode, 0.187 mgPt/cm2 with the average nanoparticle size determined by XRD of the CCM of 2.9 nm. On both side of the MEA we aligned SGL 22BB GDL, gas diffusion layer, which is a porous material that provide pathways for the reactant gases (hydrogen and oxygen) to reach the catalyst layers. Kapton subgasketing surrounding the active area of the MEA was used to to prevent gas leakage and maintain proper separation between the anode and cathode compartments[1].

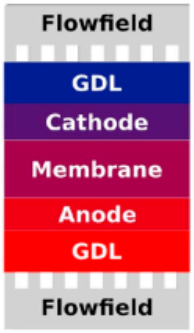

Figure 1: Schematic representation of the MEA structure [1].

2.3. High Energy X-Ray Powder Diffraction

The study was done at ID31, a dedicated beamline at the European Source Radiation Facility (ESRF) for interface and materials processing studies using high energy x-rays. Platinum nanoparticles undergoing different electrochemical processes are studied thanks to XRD technique. X-ray photons with a high kinetic energy (77 keV) are employed. A powdered sample, consists of many small crystallites randomly orientated. The investigated sample can be regarded as a collection of a huge number of scatterers, each of them, when stimulated by the incident x-ray radiation, generates a spherical wave. The spherical waves produced by the atoms of the crystal give rise to constructive interference only in some specific directions determined by the Bragg's law:

$$n\lambda = 2d\sin\theta \tag{6}$$

where d is the spacing between diffracting planes, θ is the incident angle, n is any integer, and λ is the wavelength of the beam. In our case we have a powdered sample, that consist of many small crystallites randomly orientated. This means that for a certain d_i spacing of the planes, there will be a certain number of crystallites having the correct orientation to produce constructive diffraction, all together those diffracted beams are added into concentric cones each of which corresponds to different spacing. These cones would intersect a flat detector surface as circles, known as Debye-Scherrer rings, these are a characteristic feature of diffraction obtained from powdered or polycrystalline materials. For each discrete diffraction angle 2θ the number of reflections is measured (in counts) by the detector. The position and spacing of the Debye-Scherrer rings provide valuable information about the crystalline structure of the material.

2.4. Detection system

To study the above phenomena two detectors are used.

- *CCD Si based detector PCO DiMAX*: a special fluorescence screen coupled with the ultra fast CCD (Charge-Coupled Device) Si based detector (PCO DiMAX) thanks to which we are able to measure the diffraction patterns at very high speeds (20kHz).
- *Pilatus 3X CdTe 2 M hybrid photoncounting area detector*: fast data acquisition it's possible thanks to a hybrid pixel technology, where each pixel in the detector has its own readout electronics. In our case with this detector we measured at 200Hz.

2.5. Electrochemical techniques

In electrochemical kinetics, the electrode potential is the most important variable that is controlled by the experimentalist, and the current is usually measured as the response. In this scenario is important to take into consideration one quantity that influences the measurement accuracy: the ohmic drop. By identifying the ohmic drop with $R_\Omega I$, and $V(t)$ with the potential seen by the electrode and $E(t)$ as the desired potential, we have $V(t) = E(t) + R_\Omega I$. In order to reduce the ohmic potential drop a solution is to use fuel cell, in which we have the reference

electrode as close as possible to the working electrode. Also, compensations techniques are used to determine and correct the ohmic drop. In our case to obtain the right value of the ohmic drop we measure the cell resistance by electrochemical impedance spectroscopy (EIS). The value of the resistance to be compensated can be entered manually in the compensation mode of potentiostat. The rates and mechanisms of electrochemical reactions occurring at electrodes are studied thanks to two techniques [4]:

- *Potential Step (PS)*: The working electrode is held at a stable initial potential for a period of time necessary to establish equilibrium, let's say this happens at time t<0. Then, at a time t=0, a potential step of the desired magnitude is applied with the aid of a potentiostat and the current transient is recorded. In the following table 2, a sum up of all the different potential steps done during the experiment is showed. Every step has been done following the same procedure: hold the potential at 0.35V for 1.2s then go for 5s to the potential registered in the first column of table2 and then back to 0.35V for 10 s. The second and third columns of table2 show the detector used. In particular the second column refers to the use of Pilatus 3X CdTe 2 M hybrid photoncounting area detector, detector 1 the third to the use of CCD Si based detector PCO DiMAX, detector 2.

	Scan rate	D1	D2
S1-CV_19	5V/s		x
S1-CV_20	3V/s		x
S1-CV_21	1V/s		x
S1-CV_22	700mV/s	x	
S1-CV_23	500mV/s	x	
S1-CV_24	200mV/s	x	
S1-CV_26	100mV/s	x	
S1-CV_27	50mV/s	x	

Table 1: List of the cyclic voltammetry done during the experiment.

	Voltage (V)	D1	D2
S1-steps_12	1.2	x	
S1-steps_13	1.2		x
S1-steps_14	1.2		x
S1-steps_15	0.9	x	
S1-steps_16	0.9		x
S1-steps_17	0.8	x	
S1-steps_18	0.8	x	
S1-steps_19	0.8		x
S1-steps_20	0.7	x	
S1-steps_21	0.7		x
S1-steps_22	0.6	x	
S1-steps_23	0.6		x
S1-steps_24	0.5	x	
S1-steps_25	0.5		x
S1-steps_26	0.1	x	
S1-steps_27	0.1		x

Table 2: List of the potential steps done during the experiment.

- *Cyclic Voltammetry (CV)*: The potential of the working electrode is varied linearly with time between two turning points. The potential is swept in one direction, forward scan, from an initial potential to a final potential and then reversed back to the initial potential, reverse scan. The potential sweep rate, i.e., the speed at which the potential is changed, is controlled to studying processes occurring at different velocities. In the following table 1, a sum up of all the different Cyclic Voltammetry done is showed. Every CV has been done following the same procedure: go from 0.1V to 1.2V in a scan rate registered in the first column of table1 for a minimum of 2 cycles. The second and third columns of table1 show the detector used, the notation is the same as in PS.

3. Data analysis protocol

In order to extract quantitative information from the diffraction pattern a data analysis protocol is followed. The software package pyFAI is used to perform an azimuthal integration of the

data, standing as the first step of this protocol. Once the data are integrated, we can proceed working on those data with TOPAS software, which allows the sequential analysis of powder diffraction data by performing Rietveld refinement. It can be considered an example of solving an inverse problem in crystallography. Indeed, it's about finding the crystal structure that produced the given diffraction pattern. The way of proceeding is following an iterative process that adjusts the parameters of the crystal structure model to minimize the difference between the calculated diffraction pattern and the experimental data. Once the refined parameters are obtained, time has arrived to use Python to extrapolate valuable informations from those data. A dedicated script is written for every PS and CV.

4. Results and Discussion

The refined parameters, in particular the lattice parameter, obtained from the diffraction patterns resulting from the different potential steps enunciated in the table 2, specifically those ones detected with Pilatus 3X CdTe 2 M hybrid photoncounting area detector, have been monitored and studied.The lattice parameter defines the distance between atoms. In the case of platinum's simple cubic crystal structure, this parameter directly measures the size of the unit cell, revealing the average Pt-Pt bond length and crystallographic strain. In the following, an example of the plots obtained from the refined data of the structural parameters corresponding to the PS identified as **S1-steps_12** in table 2. A dedicated script for every PS performed has been written, with the aim of calculating the time constants that characterize the change of the lattice parameter both in charging and discharging phases. We will indicate with $\Delta Lattice\ Parameter$ the change in the lattice parameter of Pt nanoparticles, in particular:

$$\Delta LatticeParameter = LP(x) - LP(0.35V) \tag{7}$$

where x is the value, in volts, of the step in potential of every PS. By modeling the EDL as a capacitor it follows that the time constants characterising its charge and its discharge are exponential. A direct way to calculate them is by determining the time constants characterizing the shift in lattice parameter. Specifically, the following equations are used, eq.8 and eq. 9.

$$y_c = \Delta LP * (1 - \exp -\frac{x_c - b_c}{\tau_{up}}) + A \tag{8}$$

$$y_d = \Delta LP * \exp -\frac{x_d - b_d}{\tau_{down}} + LP(x) \tag{9}$$

Where eq.8 describes the exponential growth of LP, y_c is the array of values of LP, ΔLP is the shift in LP, x_c is the array of values of time, τ_{up} is the charging time constant and A is the value of LP at 0,35 V. Eq. 9 describes the exponential decrease of LP, y_d is the array of values of LP, ΔLP is the shift in LP, x_d is the array of values of time, τ_{down} is the discharge time constant, LP(x) is the value of LP at the potential x, that is the potential at which the discharge starts. Those curves are perfectly fitting the shift in LP, indeed are those green exponential curves visible in the plots of fig. 3.

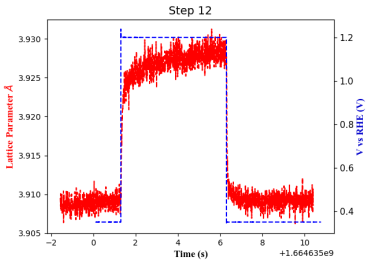

(a)

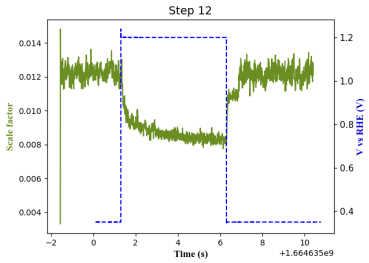

(b)

Figure 2: Lattice parameter trend (red) following the steps of the potential (blue) (a), scale factor trend (green) following the steps of the potential (blue) (b).

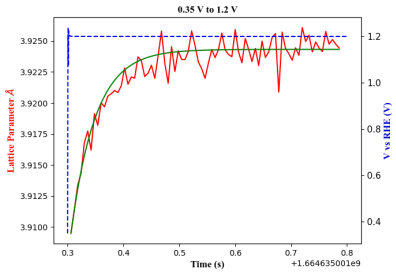

(a)

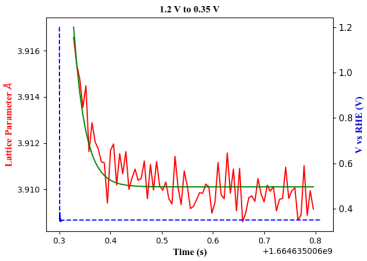

(b)

Figure 3: LP extracted from diffractograms collected stepping the potential from 0.35V to 1.2V (a) and from 1.2V to 0.35V (b). Lattice parameter(red) following the steps of the potential (blue) fitted with exponential(green).

In figure 4 two plots show the results obtained though the data analysis performed on all the PS data. In particular, the plot 4a shows the calculated values representing the time constants that characterize the change in value of the lattice parameter due to the application of a step potential, those have been estimated with eq.8 and eq.9. On blue the time constants related to the rising step, from 0,35 V to the value, in volts, indicated on the x axis and on orange the time constants related to the falling step, from the value, in volts, indicated on the x axis to 0,35 V. The minimum in shift of LP, minimum ΔLP, is typical of those PS in which the potential change just determines the reorganization of the DL, just capacitive current. The time constants characterizing the Double Layer reorganization have been calculated, the charging time constant is 0.0084 $\pm$ 0.005 s and the discharging time constant corresponds to 0.0064 $\pm$ 0.0042 s. Different time constants at different potentials are also calculated, monitoring the LP shift of different electrochemical processes happening on Pt NP surface: adsorption of oxygenated species, place exchange (PE) and adsorption of underpotentially deposited hydrogen. Evidence was given of the different kinetics involving those different phenomena, PE was confirmed to have a very slow kinetics, charging and discharging time constants are: 0.0437 $\pm$ 0.0034 s and 0.0226 $\pm$ 0.0035.

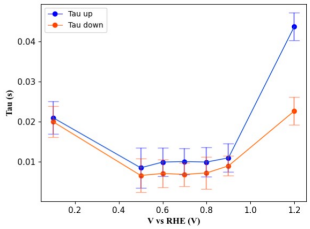

(a)

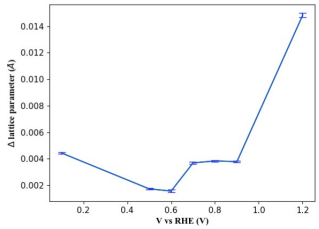

(b)

Figure 4: Graphs showing the results obtained from the PS analysis.

In the case of CV, the considered refined parameter has been the scale, which is a parameter proportional to the total number of illuminated Pt atoms in the metallic crystal lattice. The diffraction patterns resulting from the different CV enunciated in the table 1, specifically those ones detected with Pilatus 3X CdTe 2 M hybrid photoncounting area detector have been taken into account. Cyclic Voltammograms and scale plots corresponding to the different scan rates have been studied. The following figure 5, shows the refined and normalized values of scale coming from the second cycle of the CV performed at different voltage sweeps. During the first cycle, oxidation and reduction are important to get a clean surface that represents the actual catalytic properties of the catalyst. To obtain relevant electrochemical information the second cycle has to be considered. By calculating the charge accumulated and the values of the scale factor at potential 1.1V, for each of the CV studied, evidence was given on support of a very new idea regarding electrochemical surface oxidation [3]. In fig. 6 we notice that as the scan rates are faster the value of charge decreases, showing that the charge-transfer process is ki-

netically slow. Whereas the scale value, which reflects the total number of illuminated Pt atoms in the metallic crystal lattice and so reflecting the presence of oxide on the surface, is constant through the different scan rates. This demonstrate that the fast extraction process depends very little on sweep rate, which shows that the extraction is driven by potential, independently of the adsorbed species around it.

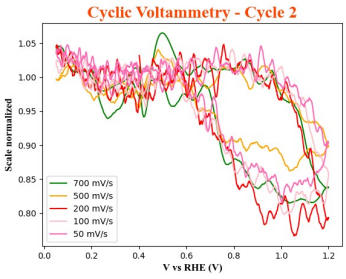

Figure 5: Graphs showing the results obtained from the CV analysis. The normalized scale values corresponding to different voltage sweeps are plotted in y axis, on x axis we find the corresponding voltage at which they have been registered.

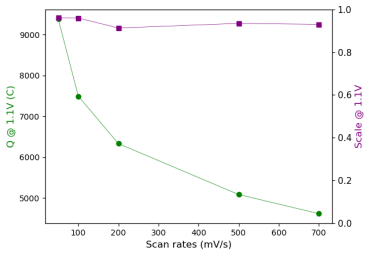

Figure 6: Charge collected in every CV considering the oxidation peak till a value of 1.1 V, in green. In purple the scale registered at 1.1V during cyclic voltammetry at various scan rates.

5. Conclusions

The development of studies aimed at understanding oxidation and reduction reactions happening on Pt-based nanocatalysts, are essential since those are key process affecting the stability and activity of Pt. Thereby directly impacting the efficiency of fuel cells. High-energy X-ray diffraction combined with PS and CV, served to study the kinetics of Pt nanoparticle surface chemistry and initial stage of metal electrooxidation. TOPAS software allowed the sequential refinement of Pt diffraction patterns collected in fast acquisition. This approach allowed the detection of lattice strain, highlighted by the lattice parameter breathing corresponding to PS. This parameter has been seen sensitive to the adsorption of electro-active species on the surface. Instead, the scale factor parameter was seen to be sensitive only to the place-exchange step in the formation of Pt oxide. This in-depth study allowed the estimation of the time constants characterizing the electric double layer restructuring and adsorption/desorption of small molecules. The CV experiments conducted in this study on Pt NP, have been done to check the validity of a innovative hypothesis made in previous study, [3], on Pt (111), in this case the aim was to explore an applied system as this nanoparticulate material. Good results were obtained but further analysis should be done. But the important take home message is that there's the necessity of recognizing the role of the electrochemical double layer in electrochemical oxidation processes, moving beyond those models focused only on solid-vacuum interface.

6. Acknowledgements

I would like to thank my supervisor Dr. Jakub Drnec and all the members of ID31 for the precious help during my internship at the ESRF and in developing the project.

References

[1] I.Martens et al. X-ray transparent proton-exchange membrane fuel cell design for in situ wide and small angle scattering tomography. *Journal of Power Sources*, 437:226906, 2019.

[2] R.Chattot et al. Electrochemical strain dynamics in noble metal nanocatalysts. *Journal of the American Chemical Society*, 143(41):17068–17078, 2021. PMID: 34623136.

[3] T.Fuchs et al. Driving force of the initial step in electrochemical pt(111) oxidation. *The Journal of Physical Chemistry Letters*, 14(14):3589–3593, 2023. PMID: 37018542.

[4] E.Santos W.Schmickler. *Interfacial Electrochemistry*. Springer Berlin, Heidelberg, Berlin, 2010.